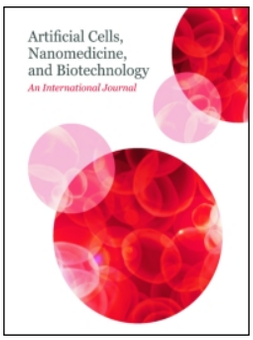

Taylor & Francis
Taylor & Francis Group

Artificial Cells, Nanomedicine, and Biotechnology
An International Journal

ISSN: 2169-1401 (Print) 2169-141X (Online) Journal homepage: http://www.tandfonline.com/loi/ianb20

A systematic study and effect of PLA/Al_2O_3 nanoscaffolds as dental resins: mechanochemical properties

Mehdi Ranjbar, Gholamreza Dehghan Noudeh, Maryam-Alsadat Hashemipour & Iman Mohamadzadeh

To cite this article: Mehdi Ranjbar, Gholamreza Dehghan Noudeh, Maryam-Alsadat Hashemipour & Iman Mohamadzadeh (2019) A systematic study and effect of PLA/Al_2O_3 nanoscaffolds as dental resins: mechanochemical properties, Artificial Cells, Nanomedicine, and Biotechnology, 47:1, 201-209, DOI: 10.1080/21691401.2018.1548472

To link to this article: https://doi.org/10.1080/21691401.2018.1548472

Published online: 19 Jan 2019.

ARTIFICIAL CELLS, NANOMEDICINE, AND BIOTECHNOLOGY
2019, VOL. 47, NO. 1, 201–209
https://doi.org/10.1080/21691401.2018.1548472

A systematic study and effect of PLA/Al_2O_3 nanoscaffolds as dental resins: mechanochemical properties

Mehdi Ranjbar[a], Gholamreza Dehghan Noudeh[a], Maryam-Alsadat Hashemipour[b] and Iman Mohamadzadeh[c]

[a]Pharmaceutics Research Center, Institute of Neuropharmacology, Kerman University of Medical Sciences, Kerman, Iran; [b]Department of Oral Medicine, School of Dentistry, Kerman University of Medical Sciences, Kerman, Iran; [c]Oral and Dental Disease Research Center, Kerman University of Medical Sciences, Kerman, Iran

ABSTRACT

One of the major and important challenges in dental composite resin and restoration is the mechanical performance and property of materials. Nanotechnology can produce nanoscale materials that are used in dentistry to help stabilize and strengthen the dentistry. In this work, we study the synthesis and characterization of PLA/Al_2O_3 nanoscaffold in different conditions such as concentration, temperature, pH, microwave power and irradiation time. PLA/Al_2O_3 nanoscaffolds were prepared by a micelle-assisted hydrothermal method. Durability, stability and biodegradable nature of nanopolymers have created the much-applied potential for using this structures in many fields such as dental resin composites. Products were characterized by X-ray diffraction (XRD), scanning electron microscopy (SEM), transition electron microscopy (TEM), Fourier transformed infrared spectrum (FT-IR), Dynamic light scattering (DLS) and atomic force microscopy (AFM). The synthesis factors were designed by Taguchi technique to control the process systematically. It was found that the intermolecular crosslinks between PLA and Al_2O_3 nanoparticles cause significant improves in the mechanical properties of PLA/Al_2O_3 nanoscaffold as dental nanocomposites. The flexural strength (88.0 MPa), modulus (7.5 GPa) and compressive strength (157.2 MPa) were calculated for PLA/Al_2O_3 nanoscaffolds loaded in Heliomolar Flow composite resins at 80 ppm (wt) concentration.

GRAPHICAL ABSTRACT

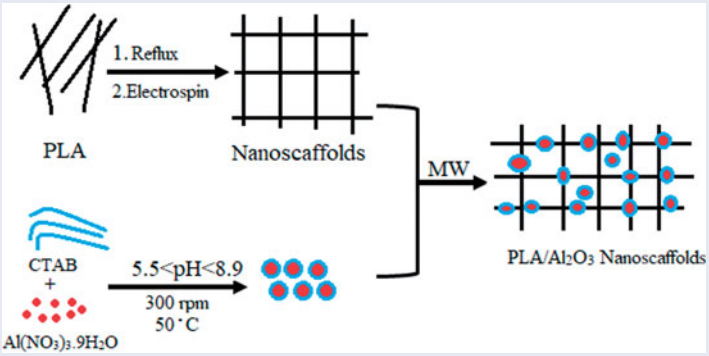

ARTICLE HISTORY
Received 8 September 2018
Revised 30 October 2018
Accepted 1 November 2018

KEYWORDS
Dental nanocomposites; PLA/Al_2O_3; crosslinking; mechanical properties

Research highlight

a. The PLA/Al_2O_3 nanoscaffolds improve mechanochemical properties of Heliomolar Flow composite resins.
b. Flowable resin composites containing 80 Wt.% nanoscaffolds show more mechanical properties.
c. Particle size of PLA/Al_2O_3 nanoscaffold composites obtained about 98–248 nm.
d. The synthesis factors were designed by Taguchi technique.

Introduction

Nanocomposites as a new material in nanotechnology science have attracted the extensive attention of researchers [1] and recent development on the market [2,3] in medicine aims at using equipment [4,5] to enhance prevention of diagnosis [6,7]. Tissue engineering [7–9], one of the important challenges in the tooth-restoration interface is polymerization shrinkage of composite resins [8,10–12], such as nanoparticles and

CONTACT Mehdi Ranjbar Mehdi.Ranjbar@kmu.ac.ir Pharmaceutics Research Center, Kerman University of Medical Sciences, P.O. Box: 76175-493, Kerman 76169-11319, Iran

Table 1. Some of extensive researches on the nanoparticles and nanocomposites as dental resin composites in recent years.

Types of nanocomposites	Purpose of use	Synthesis method	Size of nanoemulsion	References
Nano-TiO_2 particles as fillers in epoxy	Thermo-mechanical properties	Dispersion	120nm	[25]
Al_2O_3-SiO_2 fillers	Mechanical properties	Sol-gel method	60–90nm	[26]
PMMA/PHEMA	Mechanical properties	Reactive suspension	10–30nm	[27]
ZnO/Al_2O_3	Hardness Improvement	Sol-gel technique	50–70nm	[28]
Mesoporous silica fillers	Rheological properties	Mixing	110nm	[29]
Epoxy/Al_2O_3	Dielectric Properties	Coprecipitation	46nm	[30]

nanocomposites due to low molecular weight particles can solve this problem [13–15]. Nanocrystals based on dental resin composites contain filler particles with size less than 100 nm (0.1 μm) have improved restorative composite resin against wear and fracture and are claimed to provide increased aesthetics, strength and durability in dental restorative materials [16,17]. Various kinds of metallic nanoparticles such as gold (Au) [18], silver (Ag) [19] also metal-oxide nanoparticles such as iron oxide (Fe_3O_4, Fe_2O_3) [20], titania (TiO_2) [21], CuO [22], and ZnO [23] are connected for use to fabricate nanocomposite for biomedical applications. Nanocomposite with chemical cross-linked networks with three-dimensional nature has the high potential to improve the mechanical properties of the material. Nanocomposites have received considerable attention in the past 50 years, due to their exceptional promise in the wide range of applications such as dental resin [24]. In recent years many researchers have studied various methods and materials with different advantages as dental resin nanocomposites, Table 1 indicates the summary of these studies. In this research, initially using the emulsion process, complete poly lactic acid nanofibers were created separately with micelation (Critical Micelation Concentration) assisted electrospinning method then Al_2O_3 hydrophobic nanoparticles synthesized concurrently on PLA nanoscaffolds with hydrothermal method. Chemical properties such as morphological, phrase structures and distribution of particle size were characterized by the X-ray diffraction (XRD), scanning electron microscopy (SEM), Transmission electron microscopy (TEM), Dynamic light scattering (DLS) and atomic force microscopy (AFM). The nanoparticle powder was added to the resin composite homogeneously, the effect of different concentrations of PLA/Al_2O_3 composites nanoscaffolds in Heliomolar Flow composite (Ivoclar Vivadent AG, FL-9494 Schaan/Liechtenstein) as novel dental nanocomposites were studied. The mechanical properties such as flexural strength, modulus and compressive strength were compared at different concentrations of PLA/Al_2O_3 composites nanoscaffolds in Heliomolar Flow composite.

Experimental

Taguchi technique

The synthesis parameters were designed by Taguchi technique and the process control was studied systematically using ratio signal to noise. The Taguchi technique was applied for optimizing of the parameters and studying the cycle time value, microwave power and total time of irradiation on the particle size of nanocomposites. An experimental design has many advantages including saving time and laboratory costs and can also randomize clinical trial which requires careful consideration of several factors before actually doing the experiment. Based on the Taguchi technique information and the statistical results it was found that size of the products is directly related to the effect of cycle time value, microwave power and total time of irradiation (TTI).

Materials and equipment for characterization

The precursors material in this work were purely and without any impurities. Water used in this research was deionized. Cetyltrimethylammonium bromide (CTAB), $Al(NO_3)_3.9H_2O$, HCl and Dimethylformamide (DMF) were purchased from Merck company and without any purification. Polylactic (PLA) granule, 3 mm nominal granule size powder with purity >99% were purchased from Sigma-Aldrich company. The NaOH with analytical grade and Heliomolar Flow (Ivoclar Vivadent AG, FL-9494 Schaan/Liechtenstein) were purchased from an Iranian company called Kimia Elixir (Nilufar st. Khorramshahr Ave. TEHRAN , IRAN).

The PLA/Al_2O_3 nanoscaffold were characterized by X-Ray diffraction with specifications of a Rigaku D-max C III, X-ray diffractometer using Ni-filtered Cu Ka radiation. Distribution size, morphology and nanoscale pictures of products were visualized by SEM (LEO 1455VP), Transmission electron microscope (TEM) images were obtained on a Philips EM208S TEM with an accelerating voltage of 100 kV. Fourier transform infrared (FT-IR) spectra were recorded on Shimadzu Varian 4300 spectrophotometer in KBr pellets, at room temperature and wavenumber of range 400–4000 cm^{-1}. Dynamic light scattering (DLS) was used to study the NC hydrodynamic sizes. The DLS experiments were performed in room temperature with Brookhaven Instruments 90 Plus particle size analyzer in Iran. Thermal stability of the nanostructures formulations was examined by thermogravimetry analysis (TGA) curves with specifications from room temperature to 800 °C with a heating rate of 10 °C/min under an argon atmosphere using SCINCO thermal gravimeter S-100 (Seoul, Korea) and indicate a little weight about 2.5% at the temperatures around 150 °C. To study the surface distribution and porosity and the average heights of the nanoparticles, atomic force microscopy (AFM) measurements were done. AFM images were obtained with an electronic nano laboratory at the technical university of Tehran-Iran.

Preparation of poly lactic acid nanoscaffolds

At the first step poly lactic acid nanoscaffolds prepared in 200 mg (sample a), 400 mg (sample b), 600 mg (sample c) of poly lactic acid dissolved in 20 ml 1:2 DMF: water deionized in three separate beakers then the solutions were subjected

to vigorous stirring for 15 min with 300 rpm at 50 °C. These solutions were transferred into the reflux system. Afterward, the solutions were transferred into electrospinning machine with constant stirring for 30 min at 45 °C. Electrospinning set up with a high-voltage power supply capable of generating voltages up to 30 kV, was used as the source of electric field. The polymer solutions were supplied through 5 ml plastic syringe attached to a tip with an inner diameter of 0.4 mm and feed rate of the solution was controlled at 1.0 ml/h. The pieces of aluminum sheets were attached to a rotating metal drum (diameter of 6 cm) which functioned as the fibre collector and the grounding electrode. A fixed electrical potential of 15 kV was applied across the distance of 10 cm between the tip of the nozzle and the outer surface of the drum. The rotational speed of the drum was 100 rpm. The electrospun time used was 2 hours and all of the electrospinning procedures were carried out at 25 °C. After performing the tests, the system was allowed to cool to a room temperature naturally, and the obtained precipitations were collected. scanning electron microscope (SEM) images of PLA nanoscaffolds in 200 mg, 400 mg, 600 mg PLA as precursor displayed in Figure 1(a,b,c). Imaging results show an increasing concentration of nanoscaffolds and these structures are formed more uniformly and separate from each other, therefore we selected sample "c" for the next step.

Fabrication of poly lactic acid/Al_2O_3 nanoscaffolds

In the second step, 4.15 mmol of $Al(NO_3)_3.9H_2O$ was dissolved in 20 ml of deionized water in three separate beakers and then the pH was adjusted [31,32] with HCl 0.1 M and NaOH 2 M at 5.5 (sample e), 7.3 (sample f), 8.9 (sample g). The above solutions and the mixture were subjected to vigorous stirring with 300 rpm at 50 °C. After 120 min 335 mg CTAB was subsequently added to the solution until critical micelle concentration was achieved [33]. In the final step 20 mg of the polylactic acid nanoscaffold optimized and 10 ml of the above solution was loaded into the microwave Teflon container and the reaction to the production of PLA/Al_2O_3 nanoscaffolds was performed in a microwave digestion system in 600w for 15 min. After that, the final products were dried at room temperature and scanning electron microscopy was performed for all three samples. The SEM images of Al_2O_3 nanoparticles loaded on polylactic scaffolds with pH adjusted to 5.5 (sample e), 7.3 (sample f), 8.9 (sample g) shown in Figure 1(d,e,f). Imaging results show an increasing pH of Al_2O_3 with more efficiency loaded on the PLA nanoscaffolds. We did statistical studies on the formation of PLA/Al_2O_3 nanoscaffolds in microwave digestion system on parameters such as microwave irradiation, irradiation time and radiation period on the particle size of products. Scheme 1 indicates the path formation of PLA/Al_2O_3 nanoscaffolds.

Preparation of resin composites contains PLA/Al_2O_3 nanoscaffold

In the next situation after synthesized PLA/Al_2O_3 nanoscaffold, the dental resin nanocomposites were prepared with different concentrations of PLA/Al_2O_3 nanoscaffolds in Heliomolar Flow composite (Ivoclar Vivadent AG, FL-9494 Schaan/Liechtenstein). For the investigation of mechanical properties of nanostructures, we added different concentrations of PLA/Al_2O_3 nanoscaffold from 0 wt% ppm up to 100 wt% ppm in resin composite. The obtained products were placed in the oven under vacuum at room temperature for 24 h, then they were loaded in a refrigerator (4 °C).

Results and discussion

Crystal structures' properties

X-ray diffraction technique is a useful identification tool for investigating the crystallographic structure, chemical composition and physical properties of nanomaterials at room temperature. X-ray diffraction patterns of Al_2O_3 nanoparticles and PLA/Al_2O_3 nanoscaffold composites are indicated in Figure 2(a,b) respectively. The presence of peaks with the same position peaks of XRD patterns of Al_2O_3 nanoparticles in PLA/Al_2O_3 nanoscaffold composites show a crystal phase has been formed. The X-ray diffraction was measured in the range of $10 < 2\Theta < 80$. The X-ray diffraction analysis indexed as 27.1°, 34.3°, 38.8°, 59.8° and 65.2° could be in positions such as (121), (211), (201), (211) and (311). The crystallographic parameters for Al_2O_3 were a = 4.7606 A°, b = 4.7606 A°, c = 12.9940 A° and crystal system was rhombohedral. A linear equation that called Debye-Scherer can be used to measure and record the average particle sizes. According to Debay-Scherer equation particle size of PLA/Al_2O_3 nanoscaffold composites obtained about 98–250 nm (Equation 1).

$$Dv = K\lambda/\beta\cos\theta \quad (1)$$

Where; Dv is the average particle size, λ is wave length of the radiation and β is the FWHM (full width at half maximum) of the reflection peak that has the same maximum intensity in the diffraction pattern.

Morphological characteristics

During the synthesis process various parameters have a direct and indirect effect on the shapes or morphologies of nanomaterial. There is an important significant relation between the particle size of nanomaterial and their performance. SEM images of PLA and PLA/Al_2O_3 nanoscaffold composites displayed with increasing pH and raising concentration of Al_2O_3 nanoparticles loaded in nanoscaffolds by distributing more appropriate size. From scanning electron microscope images, it was understood that Al_2O_3 nanoparticles in emulsions loaded on PLA nanoscaffold by distributing a uniform particle size. Atomic Force Microscopy (AFM) has been used to measure the morphological surface properties and mechanical properties such as elastic modulus and the stiffness of the resin composites. AFM images of Al_2O_3 nanoparticles and PLA/Al_2O_3 nanoscaffold composites are shown in Figure 3(a,b). Investigation of surface morphological properties in PLA/Al_2O_3 nanoscaffold composites illustrates which PLA nanofibres are formed with a regular diameter

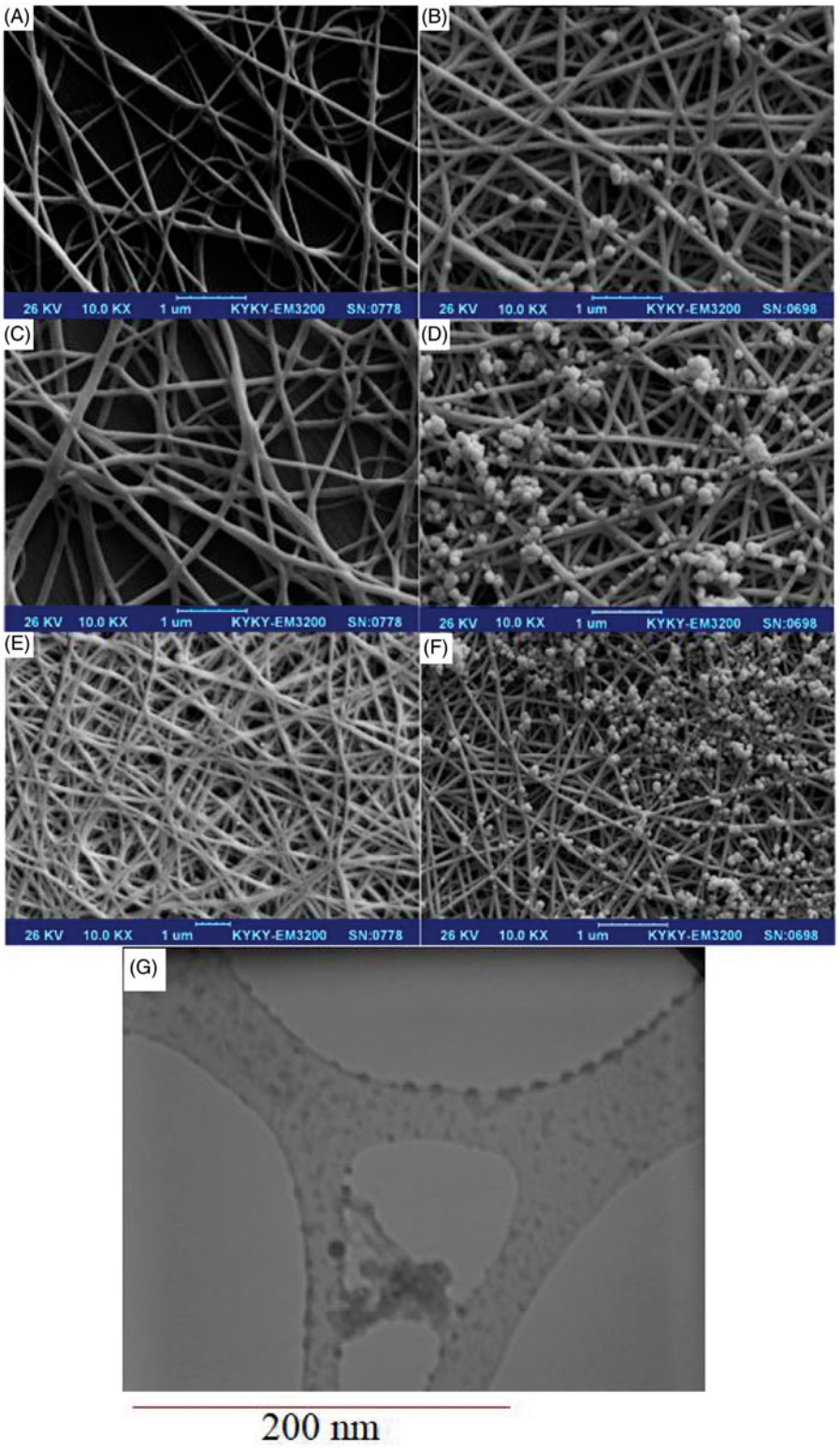

Figure 1. SEM images of polylactic acid nanoscaffold in 200 mg (A), 400 mg (B), 600 mg (C) polylactic acid, also Al_2O_3 nanoparticles loaded on polylactic acid scaffolds with pH adjusted to 5.5 (D), 7.3 (E), 8.9 (F). TEM image of Al_2O_3 nanoparticles loaded on polylactic acid nanoscaffold (G).

without any rupture. Also, PLA/Al_2O_3 nanoscaffold composites have distributed proper dispersion. Dynamic light scattering is a physical method used to determine the distribution of particles in solutions and suspensions. This non-destructive and rapid method is used to determine the particle size in the range of a few nanometers to microns. In recent technologies, particles with a diameter of less than nm can also be measured by this method. Dynamic light scattering data diagram of PLA/Al_2O_3 nanoscaffold is shown in Figure 3(c). Results show that the particle size of nanostructures in the range of 98–250 nm which have good agreement with the data obtained from scanning electron microscopy and transmission electron microscopy images. The scientific findings show high values of pH due to the

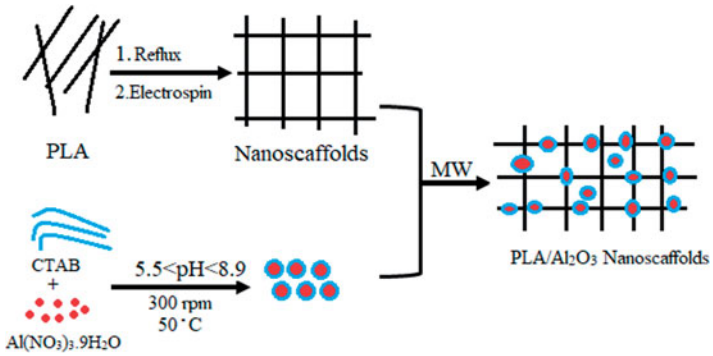

Scheme 1. Summary of the experimental route for the preparation of PLA/Al_2O_3 nanoscaffold.

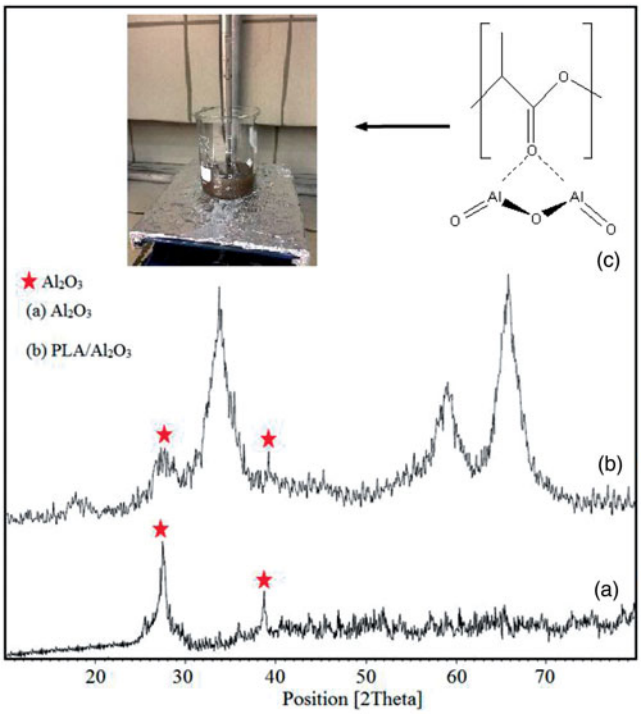

Figure 2. X-ray diffraction patterns of Al_2O_3 nanoparticles (a), and PLA/Al_2O_3 nanoscaffold composites (b), Intermolecular crosslinks between PLA and Al_2O_3 nanoparticles (c).

formation of more radical species such as $H^{\bullet}$ and $^{\bullet}OH$ on different parameters of microwave digestion system due to the formation of more nuclei the smaller nanoparticles are produced [34,35]. Fourier Transform infrared (FTIR) analysis for PLA and PLA/Al_2O_3 nanoscaffold are shown in Figure 4(a,b).

Experimental design

Signal-to-noise (S/N) ratio describes the desirable value and undesirable value for the effect of different parameters, respectively. For the measure of the quality a typical value deviating the S/N ratio value was calculated from the equation below (Equation (2,3)):

$$\frac{S}{N} = -10\mathrm{Log}(\mathrm{MSD}) \quad (2)$$

$$\mathrm{MSD} = y_1^2 + y_1^2 + y_1^2/n \quad (3)$$

Mean squared displacement (MSD) is a measure of the deviation of the position of a particle with respect to a reference position over time. where y_1, y_2, etc. are the results of experiments; n is the number of repetitions. In this research, Taguchi analysis results show cycle time value, microwave power and total time of irradiation, all three cases were the influencing parameters on the particle size and particle size distribution of PLA/Al_2O_3 nanoscaffold composites. 3 D surface plots in Figure 5 shows the effect of cycle time value, microwave power and total time of irradiation (TTI) on the size and particle size distribution of products. The results show that with increasing cycle time value and microwave power particle size becomes smaller. Table 2 indicates the upper and lower limits for each of the factors.

Mechanical properties

After performing the statistical tests, a sample with nanoscale particle size of about 220 nm due to the uniform dispersion and morphology in particles was chosen as an optimal sample and mechanical properties were investigated in combination with Heliomolar Flow composite resins. To assess the physical performance of dental resins we did flexural strength, compressive strength and modulus tests. The flexural strength tests were measured according to ISO 4049 in terms of MPa. All three-point bending was performed using a universal testing machine (Z20, Zwick Roell, Germany) at a cross-head speed of 0.5 mm min^{-1}. The Heliomolar Flow composite resins contain different concentrations of PLA/Al_2O_3 nanoscaffolds from 0 ppm up to 100 ppm wt% were compressed in the specified template with 2 mm $\times$2 mm $\times$ 25 mm dimensions, then the samples were placed in deionized water for 24 h at room temperature. Later, the final cakes were dried and all of the surfaces were polished and investigated with the universal testing machine. The flexural strength and flexural modulus histograms are shown in Figure 6(a,b) indicates by increasing the concentration of nanoparticles in the resin structures, more penetration of nanoparticles occurs in the polymeric network, which leads to the formation of stronger networks between the polymer nanoparticles during

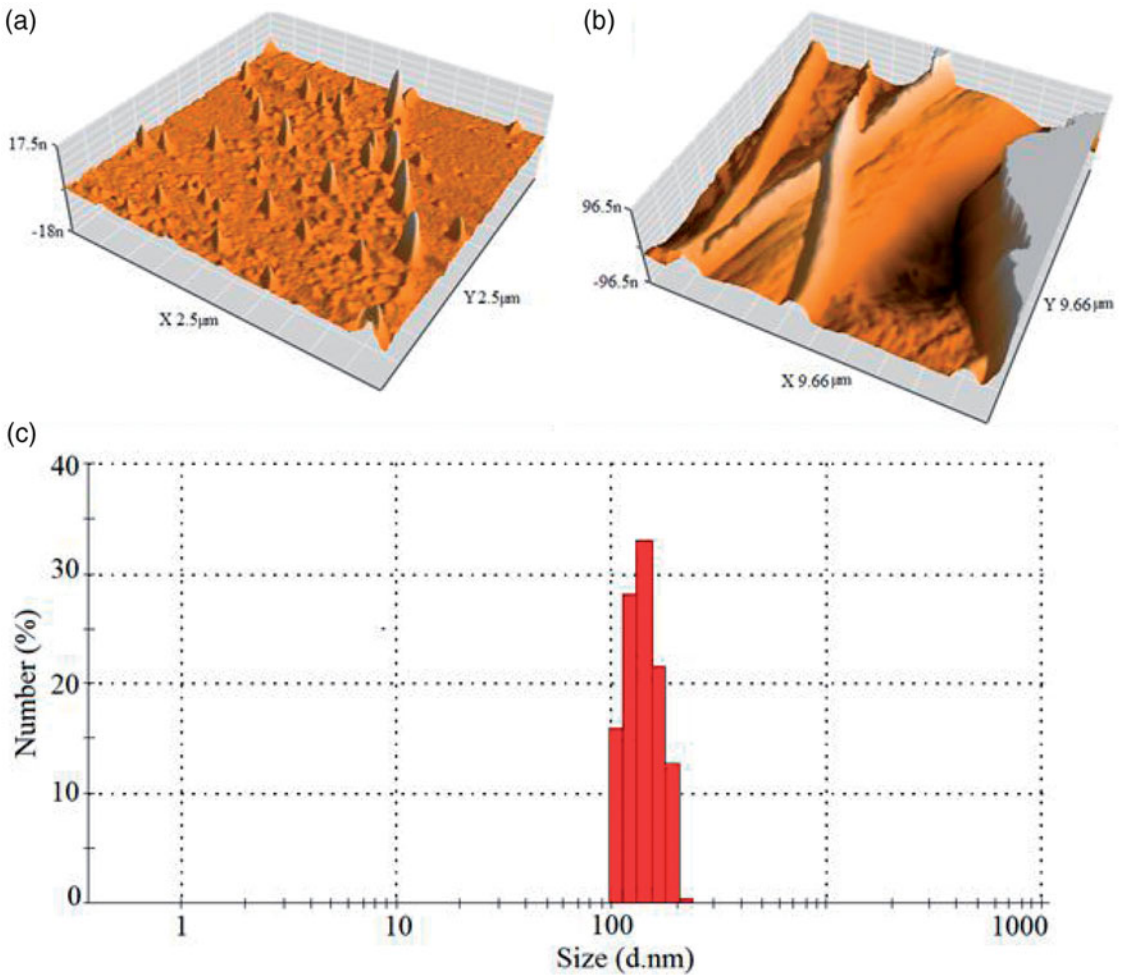

Figure 3. AFM images of Al_2O_3 nanoparticles (a), and PLA/Al_2O_3 nanoscaffold composites (b), Dynamic light scattering data diagram of PLA/Al_2O_3 nanoscaffold (c).

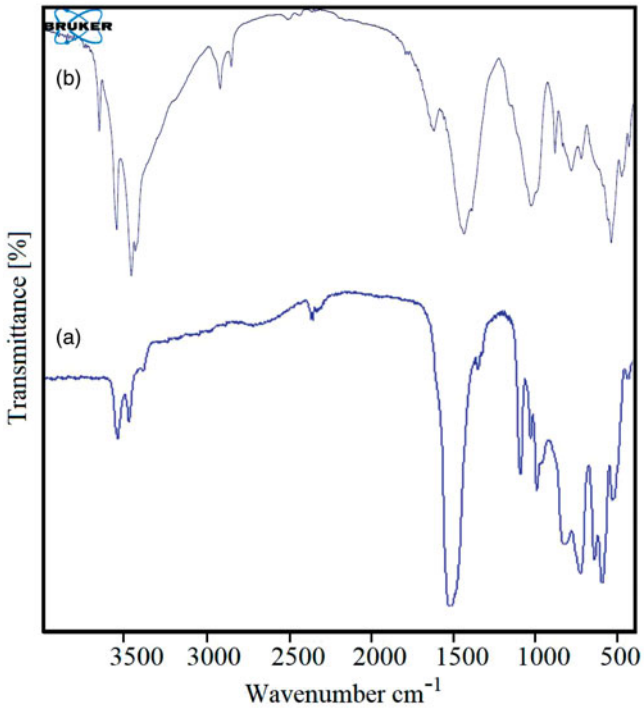

Figure 4. FT-IR spectrum of PLA [36] (a), PLA/Al_2O_3 nanoscaffold composites (b).

polymerization. The polymer nanoparticles can penetrate into the resin matrix so that the composite can be formed as an interpenetrating polymer network during the polymerization process. To measure compressive strength tests according to ISO 9917, the resin nanocomposites were compressed in the stainless steel cylindrical template with 6 mm ×4 mm dimensions then the compressive strength was determined with the universal testing machine at a cross-head speed of 1 mm min^{-1}. compressive strength tests of the Heliomolar Flow composite resins contain different concentrations of PLA/Al_2O_3 nanoscaffolds from 0 ppm up to 100 ppm wt% indicated in Figure 6(c). The results of our study indicate that the incorporation of PLA/Al_2O_3 nanoscaffolds into the resin composites have a significant effect on the mechanical properties. In this study, results show at 80 ppm (wt) concentration PLA/Al_2O_3 nanoscaffold loaded in Heliomolar Flow composite as resins, the flexural strength (88.0 MPa), modulus (7.5 GPa) and compressive strength (157.2 MPa) were calculated. With the increase in nanoscaffold concentration up to 100 ppm(wt) gradually the flexural strength, modulus and compressive strength were increased. After 80 ppm (wt) concentrate of PLA/Al_2O_3 nanoscaffold mechanical properties of dental resin composite has been decreased. The results showed that increasing the concentration of nanoscaffolds causes

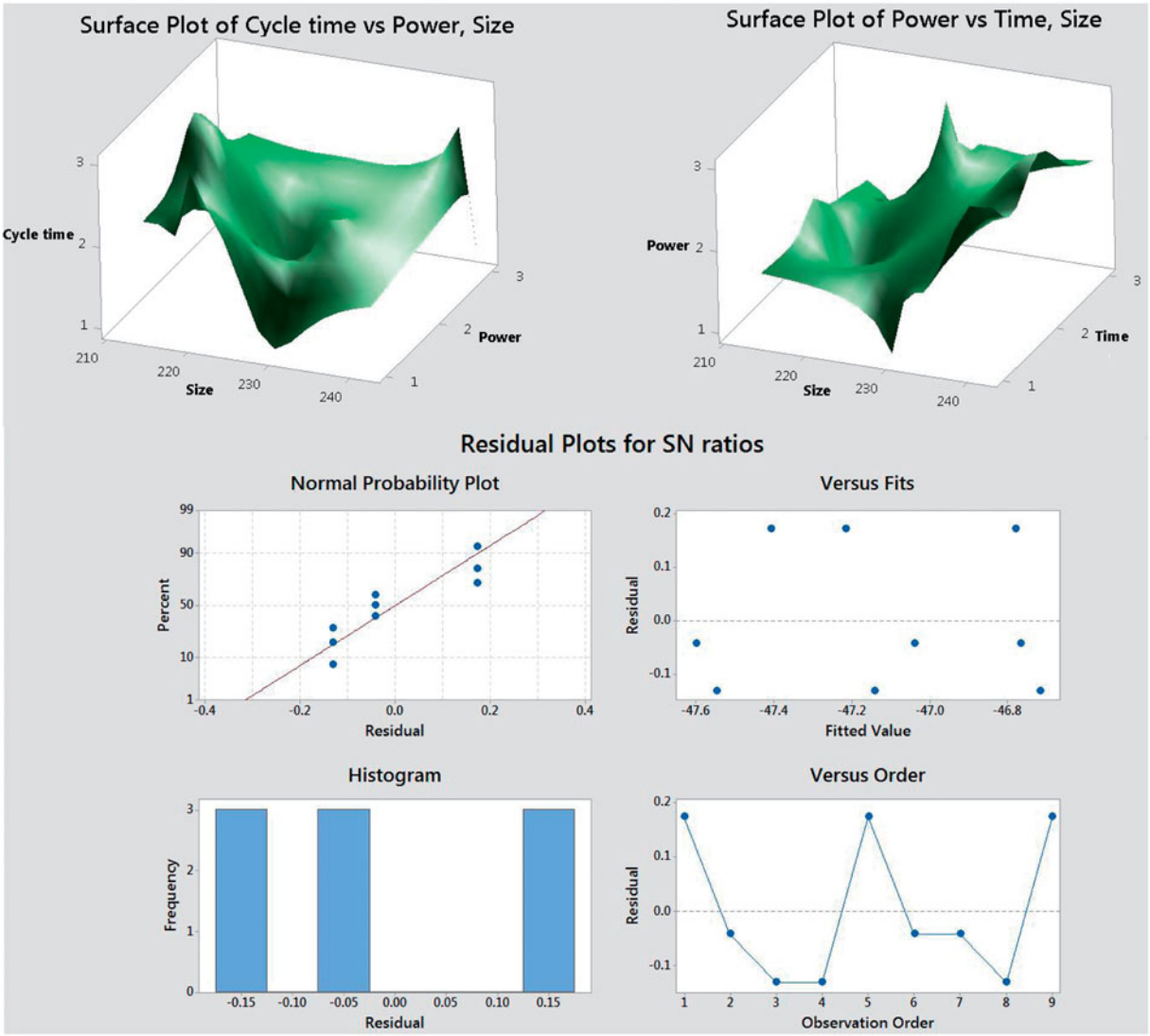

Figure 5. 3D surface plots in of cycle time value, microwave power and total time of irradiation (TTI) on the size and particle size distribution PLA/Al_2O_3 nanoscaffold composites with Taguchi technique.

aggregation in structures. This happening decreases the property of dispersion size of nanostructures in resin composite. A sudden increase in compressive strength for 20 ppm (wt) concentration is due to the lack of proper links and the presence of disturbing attractions in the nanostructures and the structure of the resin.

Table 2. The upper and lower limits for each of the factors in taguchi technique.

Range\ Factor	Low	High
TTI	5 minutes	15 minutes
Cycle time	15 second	60 second
Microwave power	600 Watt	900 Watt

Conclusion

In this work, for the first time we synthesized poly-lactic acid nanoscaffolds in three different concentrations. Then, by synthesizing nanocrystalline aluminum oxide structures in different pH, these structures were placed in polymeric structures, and optimization of aluminum nanostructures in the polymer was also performed. In this study the statistical studies of various parameters such as cycle time value, microwave power and total time of irradiation on the particle size of nanocomposites were studied. Products were characterized by X-ray diffraction (XRD), scanning electron microscopy (SEM), Transmission electron microscopy (TEM), Dynamic light scattering (DLS) and atomic force microscopy (AFM). For PLA/Al_2O_3 nanoscaffolds loaded in Heliomolar Flow composite resins at 80 ppm (wt) concentration the flexural strength, modulus and compressive strength were calculated at 88.0 MPa, 7.5 GPa (157.2 MPa) respectively.

Acknowledgements

This research did not receive any specific grant from funding agencies in the public, commercial, or not-for-profit sectors. Authors are grateful of Pharmaceutics Research Center, Institute of Neuropharmacology, Kerman University of Medical Sciences, Kerman, Iran.

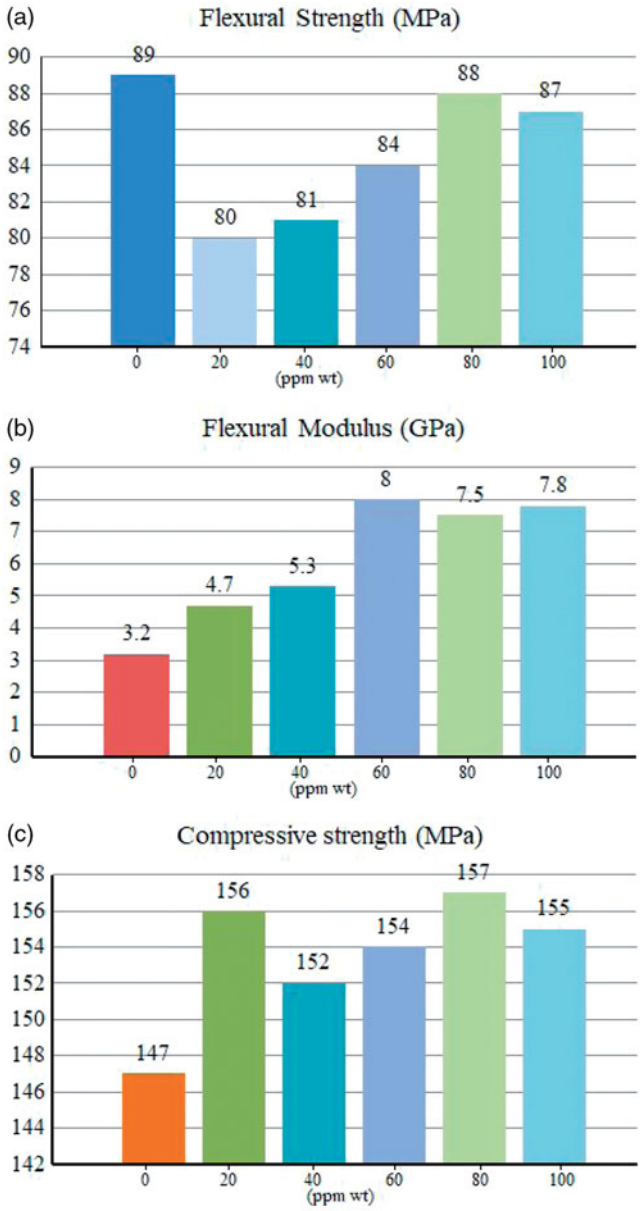

Figure 6. Mechanical properties of the final resin composites with different amounts of PLA/Al_2O_3 nanoscaffolds. (a) flexural strength (MPa); (b) flexural modulus(GPa); (c) compressive strength(MPa).

Ethical approval

This article does not contain any studies related to human or animal subjects.

Disclosure statement

No potential conflict of interest was reported by the authors.

References

[1] Al-Wahadni A, Al-Omari MA. Dental diseases in a Jordanian population on renal dialysis. Quintessence Int. 2003;34:343-347.

[2] Atai M, Pahlavan A, Moin N. Nano-porous thermally sintered nano silica as novel fillers for dental composites. Dent Mater. 2012;28:133–145.

[3] Aromaa MK, Vallittu PK. Delayed post-curing stage and oxygen inhibition of free-radical polymerization of dimethacrylate resin. Dent Mater. 2018;34:1247-1252.

[4] Makvandi P, Jamaledin R, Jabbari M, et al. Antibacterial quaternary ammonium compounds in dental materials: a systematic review. Dent Mater. 2018;34:851–867.

[5] Karabela MM, Sideridou ID. Effect of the structure of silane coupling agent on sorption characteristics of solvents by dental resin-nanocomposites. Dent Mater. 2008;24:1631–1639.

[6] Miao X, Zhu M, Li Y, et al. Synthesis of dental resins using diatomite and nano-sized SiO2 and TiO2. Prog Nat Sci Mater Int. 2012; 22:94–99.

[7] Milosevic M. Polymerization mechanics of dental composites – advantages and disadvantages. Procedia Eng. 2016;149:313–320.

[8] Ai M, Du Z, Zhu S, et al. Composite resin reinforced with silver nanoparticles–laden hydroxyapatite nanowires for dental application. Dent Mater. 2017;33:12–22.

[9] Mohamad KA, Nazanin F, Jafar SM. Synthesis and characterization of Dental Nanocomposite based on Hydroxyl Apatite/ZnO-MgO by Ultrasonic Method. Res J Chem Environ. 2013;17:53–56.

[10] Ahmadzadeh S, Rezayi M, Karimi-Maleh H, et al. Conductometric measurements of complexation study between 4-Isopropylcalix [4] arene and Cr3+ cation in THF–DMSO binary solvents. Measurement. 2015;70:214–224.

[11] Ahmadzadeh S, Rezayi M, Kassim A, et al. Cesium selective polymeric membrane sensor based on p-isopropylcalix [6] arene and its application in environmental samples. RSC Adv. 2015;5: 39209–39217.

[12] Ahmadzadeh S, Karimi F, Atar N, et al. Synthesis of CdO nanoparticles using direct chemical precipitation method: fabrication of novel voltammetric sensor for square wave voltammetry determination of chlorpromazine in pharmaceutical samples. Inorg Nano Metal Chem. 2017;47:347–353.

[13] Kumar N, Zafar MS, Dahri WM, et al. Effects of deformation rate variation on biaxial flexural properties of dental resin composites. J Taibah Univ Med Sci. 2018;13:319–326.

[14] Qasim SB, Rehman IU. Application of nanomaterials in dentistry. In Micro and nanomanufacturing. Vol 2. M.J. Jackson and W. Ahmed, editors. Cham: Springer International Publishing; 2018. p. 319–336.

[15] Wang W, et al. Structure–property relationships in hybrid dental nanocomposite resins containing monofunctional and multifunctional polyhedral oligomeric silsesquioxanes. Int J Nanomed. 2014;9:841.

[16] Xia Y, Zhang F, Xie H, et al. Nanoparticle-reinforced resin-based dental composites. J Dent. 2008;36:450–455.

[17] Yazdani J, Ahmadian E, Sharifi S, et al. A short view on nanohydroxyapatite as coating of dental implants. Biomed Pharmacother. 2018;105:553–557.

[18] Sarosi C, Biris AR, Antoniac A, et al. The nanofiller effect on properties of experimental graphene dental nanocomposites. J Adhes Sci Technol. 2016;30:1779–1794.

[19] Travan A, Marsich E, Donati I, et al. Silver–polysaccharide nanocomposite antimicrobial coatings for methacrylic thermosets. Acta Biomaterialia. 2011;7:337–346.

[20] Karthi S, Kumar GA, Sardar DK, et al. Fluorapatite coated iron oxide nanostructure for biomedical applications. Mater Chem Phys. 2017;193:356–363.

[21] Sun J, Petersen EJ, Watson SS, et al. Biophysical characterization of functionalized titania nanoparticles and their application in dental adhesives. Acta Biomaterialia. 2017;53:585–597.

[22] Stubbing J, Brown J, Price GJ. Sonochemical production of nanoparticle metal oxides for potential use in dentistry. Ultrasonics Sonochemistry. 2017;35:646–654.

[23] Khatami M, Varma RS, Zafarnia N, et al. Applications of green synthesized Ag, ZnO and Ag/ZnO nanoparticles for making clinical antimicrobial wound-healing bandages. Sustainable Chem Pharm. 2018;10:9–15.

[24] Bapat RA, Chaubal TV, Joshi CP, et al. An overview of application of silver nanoparticles for biomaterials in dentistry. Mater Sci Eng C Mater Biol Appl. 2018;91:881–898.

[25] Ambrosi A, Morrin A, Smyth MR, et al. The application of conducting polymer nanoparticle electrodes to the sensing of ascorbic acid. Analytica Chimica Acta. 2008;609:37–43.
[26] Aimin C, Chunlin H, Juliang B, et al. Antibiotic loaded chitosan bar: an *in vitro*, *in vivo* study of a possible treatment for osteomyelitis. Clin Orthop Relat Res. 1999;366:239–247.
[27] Pereda M, Ponce AG, Marcovich NE, et al. Chitosan-gelatin composites and bi-layer films with potential antimicrobial activity. Food Hydrocolloids. 2011;25:1372–1381.
[28] Dai T, Tanaka M, Huang Y-Y, et al. Chitosan preparations for wounds and burns: antimicrobial and wound-healing effects. Exp Rev anti-Infect Ther. 2011;9:857–879.
[29] Bonilla J, Fortunati E, Vargas M, et al. Effects of chitosan on the physicochemical and antimicrobial properties of PLA films. J Food Eng. 2013;119:236–243.
[30] Farhoudian S, Yadollahi M, Namazi H. Facile synthesis of antibacterial chitosan/CuO bio-nanocomposite hydrogel beads. Int J Biol Macromol. 2016;82:837–843.
[31] Khan AA, et al. Effect of different pH solvents on micro-hardness and surface topography of dental nano-composite: an *in vitro* analysis. Pak J Med Sci. 2015;31:854.
[32] Cilli R, Pereira JC, Prakki A. Properties of dental resins submitted to pH catalysed hydrolysis. J Dent. 2012;40:1144–1150.
[33] Ritacco H, Kovensky J, Fernández-Cirelli A, et al. A simplified method for the determination of critical micelle concentration. J Chem Educ. 2001;78:347.
[34] Inwati GK, Rao Y, Singh M. *In situ* free radical growth mechanism of platinum nanoparticles by microwave irradiation and electrocatalytic properties. Nanoscale Res Lett. 2016;11:458.
[35] Horikoshi S, N. Serpone . Microwaves in nanoparticle synthesis: fundamentals and applications. 1st ed. John Wiley & Sons; 2013.
[36] Wang DK, Varanasi S, Fredericks PM, et al. FT-IR characterization and hydrolysis of PLA-PEG-PLA based copolyester hydrogels with short PLA segments and a cytocompatibility study. J Polym Sci Part A: Polym Chem. 2013;51:5163–5176.